Contributed paper

OPTO-ELECTRONICS REVIEW **10**(3), 199–207 (2002)

Measurement of full-polarisation parameters using in-line fibre-optic polarimetric device

L.R. JAROSZEWICZ* and P. MARĆ

Institute of Applied Physics, Military University of Technology
2 Kaliskiego Str., 00-908 Warsaw, Poland

The in-line fibre-optic polarisation analyser enabling measurement of full polarisation parameters of light propagated in optical fibre is presented in the paper. This device uses a standard single-mode optical fibre in a system of the polarimetric configuration. Introduction of controlled birefringence in such a fibre and application of an appropriate polariser set at the end of the system allow to get full information about polarisation parameters to obtain. Evaluation of any changes of the state as well as the degree of polarisation have been achieved by application of an appropriate detection system and numerical calculation based on the coherence matrix theory. Finally, some experimental results of the system performance and determination of the main errors are presented.

Keywords: fibre-optic sensor, polarimeter, state and degree of polarisation.

1. Introduction

The possibility of measuring the full light polarisation parameters, i.e., state of polarisation (SOP) and degree of polarisation (DOP) in bulk-optics is well known and has been developed for many years. Such systems are used in spectro-polarimetry [1], in automatic recognition of target images [2-4], and sensor areas [5]. However, the methods of SOP and DOP determination by fibre-optic systems are relatively new. As a matter of fact there were presented in the literature fibre-optic polarimetric systems [6] but it was not used for determination of polarisation properties of light. The first works presenting methods of SOP measuring by in-line optical fibre system were published in Refs. 7 and 8. An in-line version of such a system giving full information about polarisation parameters (i.e., ellipse and degree of polarisation) of the investigated light is presented in this paper. The first theoretical description of in-line fibre-optic system allowing investigation of full polarisation parameters was introduced in Ref. 9. This theory has been used as a base for the system described in this paper.

The principle of operation is based on birefringence modulation in the standard single-mode fibre and a suitable detection of harmonic amplitudes from the output electric signal. In order to introduce controlled birefringence modulation in the optical fibre, the piezoceramic squeezer has been used. From theoretical point of view this element works as a linear phase shifter (LPS) whose principle of operation is schematically shown in Fig. 1. Modulated light goes through the polariser and is detected by the photodetection system. The output time-depended electric signal carries information about all searched polarisation parameters of light in its harmonic amplitudes. It should be noticed that the above presented idea of the LPS element performance has been firstly presented in Ref. 8.

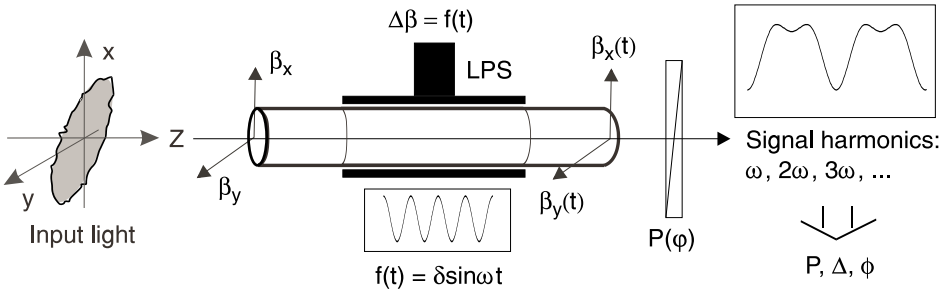

Fig. 1. Main idea of the linear phase shifter (LPS) application for determination of polarisation parameters.

*e-mail: jarosz@wat.waw.pl

2. In-line fibre-optic polarisation analyser – system arrangement and description of operation

2.1. Theoretical description of different light polarisation parameters

The full polarisation description of the light propagating through any optical system requires consideration of its statistical properties; hence it has been assumed that light is quasi-monochromatic and partially polarised. For light description, the coherence matrix $\boldsymbol{J}$ approach in the following form has been used [10]

$$\boldsymbol{J} = \begin{bmatrix} \langle E_x^* E_x \rangle & \langle E_y^* E_x \rangle \\ \langle E_x^* E_y \rangle & \langle E_y^* E_y \rangle \end{bmatrix} = \begin{bmatrix} J_{xx} & J_{xy} \\ J_{yx} & J_{yy} \end{bmatrix}, \tag{1}$$

where

$$\langle \ldots \rangle = \lim_{T \to \infty} \frac{1}{2T} \int_{-T}^{T} (\ldots)\, dt$$

denotes time averages, symbol „*" denotes complex conjugation, and E_x, E_y denote two orthonormal electric field vector components that are perpendicular to the direction of light propagation.

Attractiveness of the above matrix is connected with its usefulness for description of optical system because the optical intensity I observed at any optical system output is equal to the trace of the output coherence matrix $\boldsymbol{J}_{out}$ [10], hence

$$I = Tr(\boldsymbol{J}_{out}), \tag{2}$$

where the output coherence matrix is connected with its form before the system $\boldsymbol{J}_{in}$ and Jones matrix $\boldsymbol{M}$ of all system [11] according to the following relation [10]

$$\boldsymbol{J}_{out} = \boldsymbol{M} \cdot \boldsymbol{J}_{in} \cdot \boldsymbol{M}^{\dagger}, \tag{3}$$

where † indicates the Hermitian-conjugate.

Remarkable fact is that $\boldsymbol{J}$ matrix gives directly information about DOP, because a total intensity of the quasi-monochromatic beam I_0 can be treated as a sum of the polarised light intensity I_P and the depolarised light intensity I_D. Thus, the DOP is characterised by the polarised light I_P to the total light I_0 intensity ratio. According to the definition of the coherence matrix, Eq. (1), this value takes the form [10]

$$P = \frac{I_P}{I_0} = \sqrt{1 - \frac{4 \det(\boldsymbol{J})}{Tr(\boldsymbol{J})^2}}. \tag{4}$$

For this reason, the DOP of polarised light is equal to 1 (P = 1), the depolarised light has DOP equal to 0 (P = 0), and all intermediate DOPs of light range between zero and one ($0 < P < 1$).

The coherence matrix contains also information about SOP describing an ellipse of the electric field vibration in a plane perpendicular to the direction of wave propagation. The SOP defined for monochromatic and polarised light beam can be described by two parameters (ϕ, Δ) of so-called standard Jones vector $\boldsymbol{E}$ as [11]

$$\boldsymbol{E} = \begin{bmatrix} \boldsymbol{E_x} \\ \boldsymbol{E_x} \end{bmatrix} = \begin{bmatrix} E_x e^{i\delta_x} \\ E_y e^{i\delta_y} \end{bmatrix} = \begin{bmatrix} \cos\phi \\ \sin\phi\, e^{i\Delta} \end{bmatrix}, \tag{5}$$

where

$$\phi = \text{arc tg}[E_y / E_x],\ \Delta = \delta_y - \delta_x,$$

$$0 \le \phi \le \frac{\pi}{2},\ 0 < \delta < 2\pi$$

and E_y, E_x, δ_x, δ_y are the amplitudes and phases of electric field components, respectively.

Consequently, the coherence matrix which describes the quasi-monochromatic and partially polarised light beam can be expressed by its intensity I_0, degree of polarisation P, and SOP parameters (ϕ, Δ) in the following form [9]

$$\boldsymbol{J}[P, \phi, \Delta] = \frac{1}{2} I_0 \begin{bmatrix} 1 + P\cos 2\phi & P\sin 2\phi e^{-i\Delta} \\ P\sin 2\phi e^{i\Delta} & 1 - P\cos 2\phi \end{bmatrix}. \tag{6}$$

This relation is the way for a description of all polarisation properties of light beam as it is done in the next part of the paper.

2.2. General theoretical system description

The construction scheme of the system called fibre-optic polarisation analyser (FOPA) is shown in Fig. 2. The optical part of this system consists of two 50–50 fibre couplers (FC-1, FC-2), LPS element, three polarisation controllers (PC1, ..., PC3) and two fibre-optic polarisers (P[0], P[π/4]). The light with unknown polarisation parameters (DOP and SOP) passes through the fibre coupler FC-1. The first FC-1 output arm is called reference arm and allows measuring of total intensity of the incoming light via detector D0. In the second arm, called signal arm, the polarisation parameters of incoming light are searched using a LPS element. Then, the light is divided by coupler FC-2 and passes through two polarisers (P[0], P[π/4]) oriented at the angle 0 and π/4 with respect to the fast axis of the LPS. Electric signals from detectors D1 and D2 are collected in personal computer after processing by lock-in amplifier. Polarisation parameters are calculated basing on these data. Additionally, three polarisation controllers are used for proper system adjusting; the first one, PC1 compensates the birefringence of the fibre before LPS, while the PC2, PC3 are used for the fibre polarisers adjusting. FOPA system is similar to the previously presented FOPE one [9], but application of the reference arm to the detection of the total light intensity as

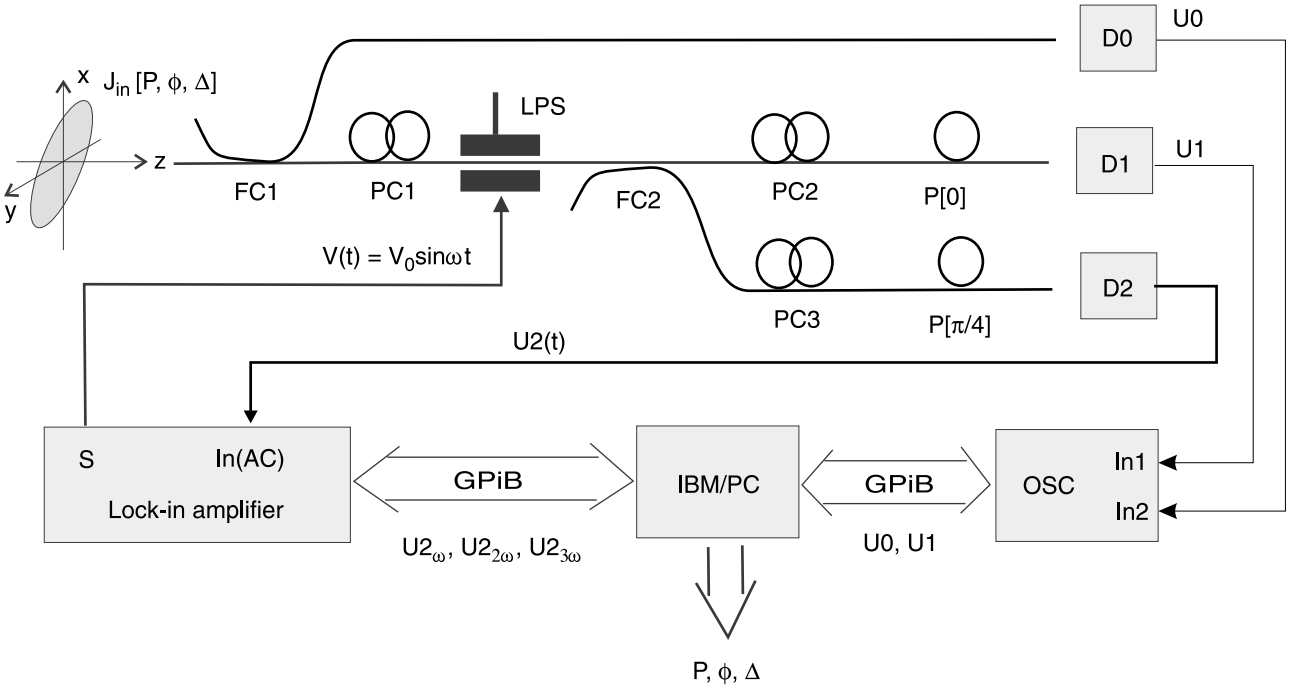

Fig. 2. General scheme of FOPA system.

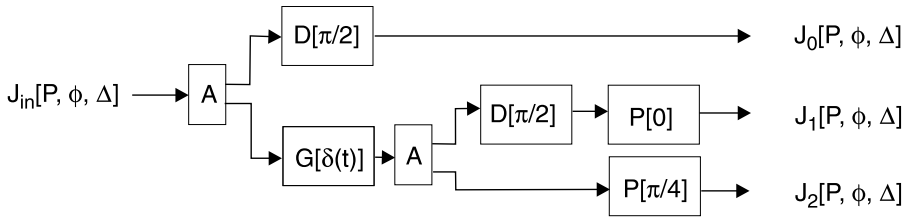

Fig. 3. The dependence between input and output coherence matrices for FOPA, described in Jones matrix approach.

well as introduction of and the new theoretical approach give a possibility of the DOP measuring, too.

To apply the coherence matrix approach to FOPA description one should know the Jones matrix form of the whole optical part. The equivalent lumped elements representation of FOPA optical part for this description is shown in Fig. 3.

The system contains three optical branches, which matrix description, i.e., $\boldsymbol{M}_0$, $\boldsymbol{M}_1$, $\boldsymbol{M}_2$, have the following form

$$\begin{aligned} \boldsymbol{M}_0 &= \boldsymbol{A}\cdot\boldsymbol{D}[\pi/2], \\ \boldsymbol{M}_1 &= \boldsymbol{P}[0]\cdot\boldsymbol{A}\cdot\boldsymbol{G}[\delta(t)]\cdot\boldsymbol{A}\cdot\boldsymbol{D}[\pi/2], \\ \boldsymbol{M}_2 &= \boldsymbol{P}[\pi/2]\cdot\boldsymbol{A}\cdot\boldsymbol{G}[\delta(t)]\cdot\boldsymbol{A}, \end{aligned} \tag{7}$$

where $\boldsymbol{P}[\phi]$ is the Jones matrix describing polariser oriented at the angle ϕ with respect to the fast axis of the LPS, $\boldsymbol{A}$ is the matrix form of the ideal coupler, $\boldsymbol{G}[\delta(t)]$ is the matrix of linear retarder describing the LPS action, and $\boldsymbol{D}[\pi/2]$ is the matrix of a constant phase retarder connected with the phase shift between two output branches of an ideal coupler [12]. The above matrices can be defined as follows [13]

$$\boldsymbol{P}[\varphi] = \begin{bmatrix} \cos^2\varphi & \sin\varphi\cos\varphi \\ \sin\varphi\cos\varphi & \sin^2\varphi \end{bmatrix}, \tag{8}$$

$$\boldsymbol{A} = \frac{1}{\sqrt{2}}\begin{bmatrix} 1 & 0 \\ 0 & 1 \end{bmatrix}, \tag{9}$$

$$\boldsymbol{D}[\eta] = \exp[-j\eta]\begin{bmatrix} 1 & 0 \\ 0 & 1 \end{bmatrix}, \tag{10}$$

$$\boldsymbol{G}[\delta(t)] = \exp[j\delta(t)/2]\begin{bmatrix} 1 & 0 \\ 0 & e^{-j\delta(t)} \end{bmatrix}, \tag{11}$$

where $\delta(t)$ is a time-dependent birefringence generated in LPS. If a voltage signal driving the piezoceramic squeezer is $V(t) = V_0 sin\omega t$, the phase changes (for linear range of SOP modulator operation [8]) is $\delta(t) = \delta_0 sin\omega t$, where δ_0 is the birefringence modulation amplitude and ω is the signal frequency.

Application of Eqs. (7–11) for calculation of the output signals $U0$, $U1$ and $U2(t)$, as well as Eqs. (2), (3), and (6) leads to the following relations

$$\begin{aligned} U0 &\cong Tr(\boldsymbol{J}_0) = Tr(\boldsymbol{M}_0 \cdot \boldsymbol{J}_{in} \cdot \boldsymbol{M}_0^{\dagger}) = \frac{1}{2} I_0 \\ U1(t) &\cong Tr(\boldsymbol{J}_1) = Tr(\boldsymbol{M}_1 \cdot \boldsymbol{J}_{in} \cdot \boldsymbol{M}_1^{\dagger}) = \frac{1}{4} I_0 (1 + P\cos 2\phi), \\ U2(t) &\cong Tr(\boldsymbol{J}_2) = Tr(\boldsymbol{M}_2 \cdot \boldsymbol{J}_{in} \cdot \boldsymbol{M}_2^{\dagger}) = \\ &= \frac{1}{4} I_0 \{1 + P\sin 2\phi \cos[\delta(t) - \Delta]\} \end{aligned} \tag{12}$$

Consequently, the output signals in FOPA system take the form

$$\begin{aligned} U0 &= U_{00} \\ U1 &\cong U_{01}(1 + P\cos 2\phi) \\ U2(t) &\cong U_{02}\{1 + P\sin 2\phi \cos[\delta(t) - \Delta]\} \end{aligned} \quad . \tag{13}$$

As one can see, only the signal from detector D2 is time-dependent and it can be expressed by the following harmonic components

$$\begin{aligned} U2(t) &= U_{02} + U_{02} P \sin 2\phi \cos \Delta \\ &\times \left[J_0(\delta_0) + 2 \sum_{k=1}^{\infty} J_{2k}(\delta_0) \cos[2k(\omega t + \varphi)] \right] + \\ &+ U_{02} P \sin 2\phi \sin \Delta \\ &\times \left[2 \sum_{k=0}^{\infty} J_{2k+1}(\delta_0) \sin[(2k+1)(\omega t + \varphi)] \right]. \end{aligned} \tag{14}$$

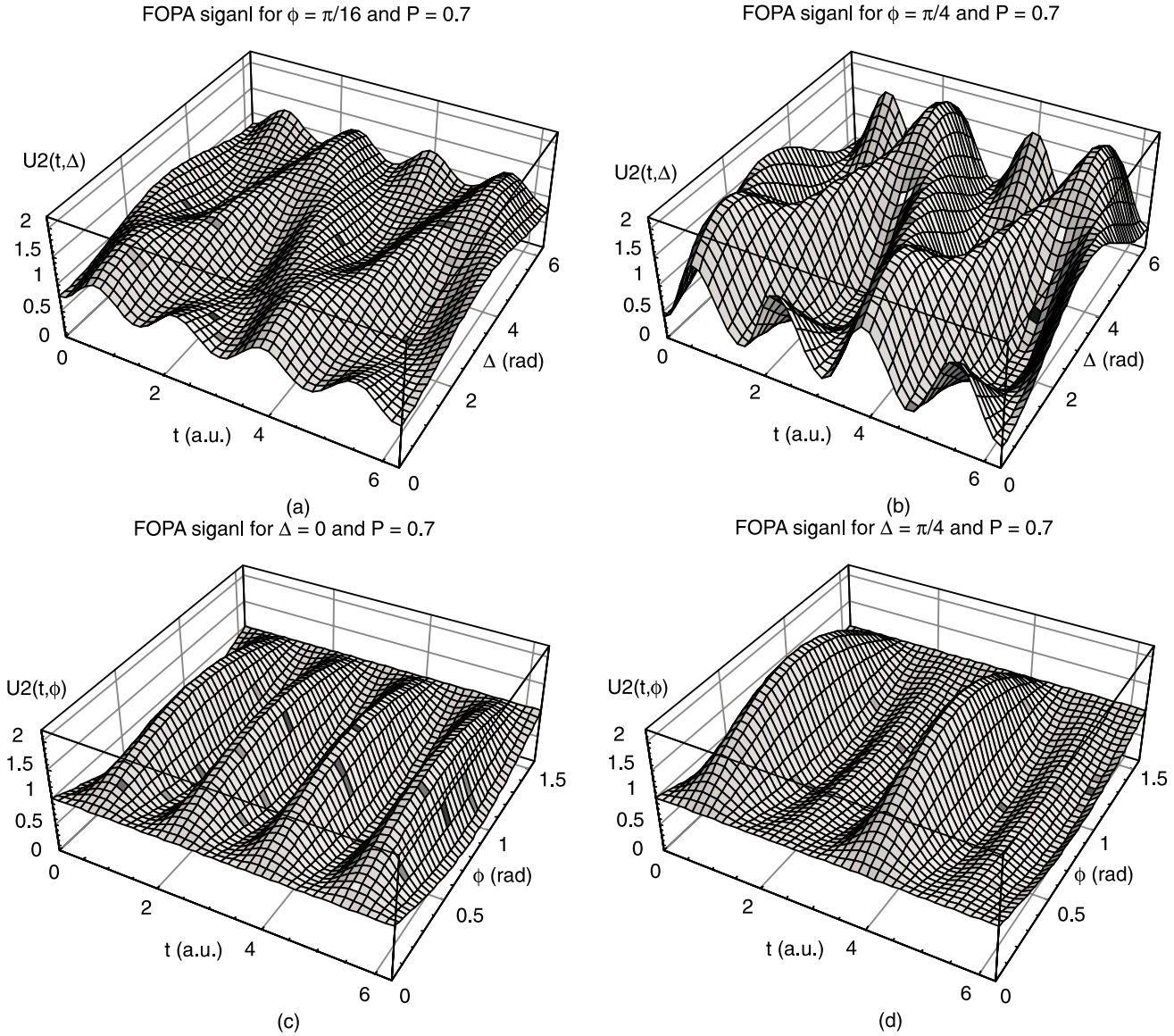

Fig. 4. Numerical simulation of the output signal $U2(t)$ for different parameters of SOP. The DOP = 0.7 has been used as a parameter for all simulation. (a) and (b) show influence of Δ for $\phi = \pi/16$ and $\phi = \pi/4$, respectively, whereas (c) and (d) influences of ϕ for $\Delta = 0$ and $\Delta = \pi/4$, respectively.

Investigation of the above relation by simulation methods (*Mathematica 4.1*, Wolfram Co.) is shown in Fig. 4. Fundamental influence of the investigated polarisation parameters on the output signals has been used in the signal processing unit. The changes of the angle ϕ generally affect the signal amplitude [compare Fig. 4(c) and Fig. 4(d)], whereas changes of Δ affect the signal harmonic ratio [compare Fig. 4(a) and Fig. 4(b)]. Moreover, the increasing DOP value increases the values amplitude of the time dependent signal $U2(t)$, as it is shown in Fig. 5.

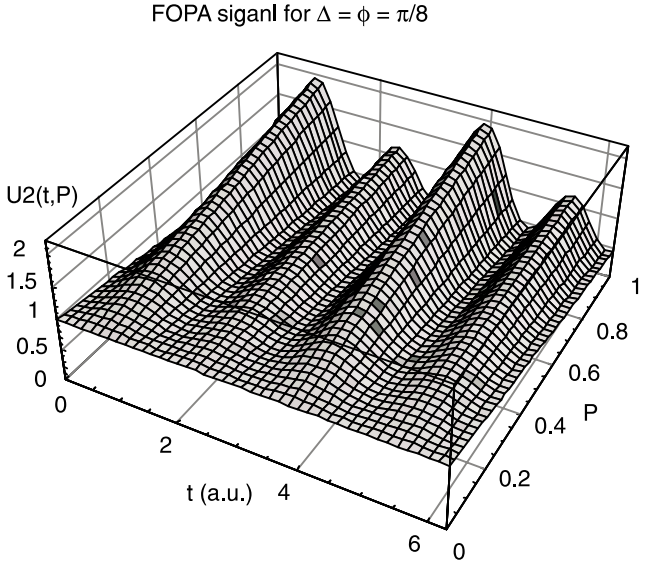

Fig. 5. Numerical simulation of the output signal $U2(t)$ for different DOP. The constant SOP with $\Delta = \phi = \pi/8$ has been used as a parameter.

The proper system performance requires the condition $J_0(\delta_0) = 0$ to be fulfilled [7,8], so the modulation amplitude δ_0 generated by the LPS must be equal to 2.4048. In this way, only the first three harmonic components of the signal from detector D2 are important and relations for the output signals take the following form

$$\begin{aligned} U0 &= U_{00} \\ U1 &= U_{01}(1 + P\cos 2\phi) \\ U2(t) &= U_{02}\left[1 + U2_{\omega}\sin\omega t + U2_{2\omega}\sin\left(2\omega t + \pi/2\right)\right. \\ &\quad \left. + U2_{3\omega}\sin 3\omega t\right] \end{aligned} \tag{15}$$

where

$$\begin{aligned} U2_{\omega} &= 2PJ_1(\delta_0)\sin 2\phi\sin\Delta \\ U2_{2\omega} &= 2PJ_2(\delta_0)\sin 2\phi\cos\Delta, \\ U2_{3\omega} &= 2PJ_3(\delta_0)\sin 2\phi\sin\Delta \end{aligned} \tag{15a}$$

Because the signal $U1$ depends directly on U_{01}, special adjusting procedure should be introduced. The main purpose of this procedure is determination of U_{01} value as it has been described in section 3.1. Finally, the parameters describing polarisation of light beam can be find from Eq. (15)

$$\begin{aligned} \Delta &= \text{arc tg}[\kappa] \\ \phi &= \frac{1}{2}\,\text{arc ctg}\,[\chi] \\ P &= \frac{|U1 - U_{01}|}{U_{01}}\sqrt{1 + \frac{1}{\chi^2}} \end{aligned} \tag{16}$$

where

$$\begin{aligned} \kappa &= \frac{J_2(\delta_2)|U2_{\omega}|}{J_1(\delta_0)|U2_{2\omega}|} \\ \chi &= 2J_1(d_0)\frac{U_{02}}{U_{01}}\frac{|U1 - U_{01}|}{|U2_{\omega}|}\frac{\kappa}{\sqrt{1+\kappa^2}} \end{aligned} \tag{16a}$$

The above relations show, that the angle Δ is determined only from appropriate amplitude ratio of the first and second harmonics of the signal $U2(t)$. Estimation of the Δ and ϕ in all ranges of their changes, (i.e., from 0 to 2π and from 0 to $\pi/2$, respectively) needs an appropriate determination of arguments of $sin\Delta$ and $cos\Delta$ trigonometric functions. These values are determined by identification of $U2_{\omega}$ and $U2_{2\omega}$ signal signs following the procedure shown in Table 1.

Table 1. Procedure of determination of an argument value for Δ.

Sign of $U2_{\omega}$	plus	plus	minus	minus
Sign of $U2_{2\omega}$	plus	minus	minus	plus
Range of angle Δ	$(0, \pi/2)$	$(\pi/2, \pi)$	$(\pi, 3\pi/2)$	$(3\pi/2, 2\pi)$

The next parameter describing SOP, i.e., the angle ϕ, can be found from the signal $U1$ and the harmonic $U2_{\omega}$ values. The degree of polarisation can be found from the signal $U1$ or other values of the first three harmonics of the signal $U2(t)$. Because the DOP is reciprocal to the angle ϕ, when ϕ is nearly zero, the DOP value is non-determinable from the mathematical point of view. For such a situation, the DOP can be determined from the signal $U1$ as a half of peak-peak value of this signal existing for changes of SOP by PC1 [see the first relation in Eq. (15)].

The proper FOPA operation needs a compensation of birefringence introduced by the optical fibre before LPS. A typical polarisation controller (PC1 – see Fig. 2) secures this operation. According to the Kapron rule of equivalence [14], the general description of any piece of standard single-mode optical fibre in Jones matrix formalism has a following form [15]

$$\boldsymbol{M}_F = \boldsymbol{R}[\Omega]\cdot\boldsymbol{G}[\delta]\cdot\boldsymbol{R}[\Phi], \tag{17}$$

If the polarisation controller is used for compensation of this birefringence, the following relation should be fulfilled

$$\boldsymbol{M}_{PC} \cdot \boldsymbol{M}_F \equiv \boldsymbol{I} \Rightarrow \boldsymbol{M}_{PC} = \boldsymbol{R}[-\Phi] \cdot \boldsymbol{G}[-\delta] \cdot \boldsymbol{R}[-\Omega]. \quad (18)$$

Analysing the results of the polarisation controller influence [12], a conclusion can be drown that it is possible to transform any SOP to the desired one by suitable changes of the angle position of two fibre loop of this device. Therefore the matrix form of this device $\boldsymbol{M}_{PC}$ generally fulfilled Eq. (18). Equation (15) shows that determination of the polarisation parameters needs only two first harmonics of the output signal $U2(t)$. The third amplitude harmonic, existing in Eq. (15), is used for estimation of the appropriate modulation amplitude ($\delta_0 = 2.4048$). This procedure is based on the operation in such a point where the ratio first-to-third harmonics gives constant value. It has been widely described in Refs. 7 and 8.

3. Experimental results

3.1. Construction and calibration of FOPA system

General view of the laboratory constructed FOPA system is shown in Fig. 6(a). A standard single-mode fibre with $\lambda_c = 610$ nm has been used. From this reason, the special couplers and polarisers made in the Applied Physics Division, the part of the Institute of Applied Physics MUT, have been applied. Because such a fibre-optic system is generally very sensitive to temperature fluctuations [16], a loose tube has been used for additional fibre protection. A piezoceramic squeezer working at about 100 V and frequency about 1.5–2 kHz has been used as the LPS [see Fig. 6(b)]. Interaction length of the optical fibre was about 5 mm and generally this interaction has not been optimised. The EG&G 7260 lock-in amplifier has been used as the digital signal processing unit. As the output signal from this device the amplitude of the first three harmonics of the signal has been taken. Additionally, the lock-in amplifier has given the intensity-normalised factor U_{02} as the integral of $U2(t)$ signal equal to ten multiplicities of the period $2\pi/\omega$. The same device has been also used for the LPS control and driving. Additionally, the system contained personal computer with a special software for a visualisation of the output signals from the electronic part as well as presentation of the calculated polarisation parameters of light in real time.

According to theoretical investigation discussed in the previous section, the input fibre birefringence is compensated by PC1. It can be easily shown that if the SOP of the light reaching the LPS is linear to the direction of the main axes of birefringence introduced by this device, no modulation of the output signals from FOPA system is observed. It is the main idea of the proper system adjustment via PC1. For this reason the polarised light with linear SOP is used

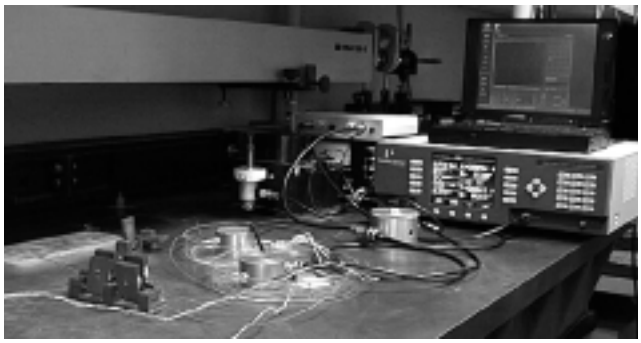

(a)

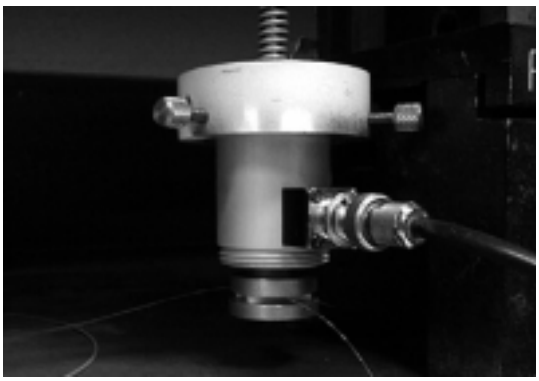

(b)

Fig. 6. General view of the FOPA system (a) and the used LPS element (b).

for system calibration. It may be a classical He-Ne laser with a rotator on the output. In the first step, the compensation of the input fibre birefringence is made. This is obtained for such a PC1 position, where signal modulation vanishes at the system output for two orthogonal input SOPs. In the second step, the input SOP is rotated by $\pi/4$, and the output polariser positions are adjusted via controllers PC2 and PC3, i.e, the second harmonic of modulation frequency at D2 and constant signal component at D1 are obtained.

The same source is used for determination of U_{01} value needed for polarisation parameter calculation via Eq. (15). For the light with linear polarisation and the angle ϕ equal to $\pi/4$, the output signals take the form

$$\begin{aligned} U0 &= U_{00}^{adj} \\ U1 &= U_{01}^{adj} \\ U2(t) &= U_{02}^{adj}[1 \pm 2Pj_2(\delta_0)\cos(2\omega t)] \end{aligned}, \quad (19)$$

where the constant U_{02}^{adj} is defined as integration of the signal $U2(t)$ in time equal to multiplicities of the period $T = 2\pi/\omega$

$$U_{02}^{adj} = \frac{1}{nT} \int_{t1}^{t1+nT} U2(t)dt, \quad n \in N. \quad (20)$$

As a result, the reference signal $U0$ equal to the constant U_{00}^{adj} is used as a normalisation factor for $U1$ and $U2$ signals. After adjusting procedure, the following normalisation quantities are obtained

$$\xi_{01} = \frac{U_{01}^{adj}}{U_{00}^{adj}}, \quad \xi_{02} = \frac{U_{02}^{adj}}{U_{00}^{adj}}. \tag{21}$$

The above relations give also normalisation factor for the signals $U1$ and $U2$ which take the final form

$$\begin{aligned} &U_1^N = \xi_{01}(1 + P\cos 2\phi), \\ &U_2^N(t) = \xi_{02} \times \\ &\times\left[1 + U2_\omega \sin\omega t + U2_{2\omega}\sin\left(2\omega t + \frac{\pi}{2}\right) + U2_{3\omega}\sin 3\omega t\right] \end{aligned} \tag{22}$$

Applying the normalisation procedure one can present the polarisation parameters described by Eq. (16) as

$$\begin{aligned} \Delta &= \text{arc tg}[\kappa] \\ \phi &= \frac{1}{2}\text{arc ctg}[\varsigma] \\ P &= \frac{\left|U1^N - \xi_{01}\right|}{\xi_{01}}\sqrt{1 + \frac{1}{\varsigma^2}} \end{aligned}, \tag{23}$$

where

$$\begin{aligned} k &= \frac{J_2(\delta_0)\left|U2_\omega\right|}{J_1(\delta_0)\left|U2_{2\omega}\right|} \\ \varsigma &= 2J_1(\delta_0)\frac{\xi_{02}\left|U1^N - \xi_{01}\right|}{\xi_{01}\left|U2_\omega\right|}\frac{\kappa}{\sqrt{1+\kappa^2}} \end{aligned}. \tag{23a}$$

3.2. Experimental research

The experimental verification of the FOPA performance has been done using the system described above. For this reason, the light of various input SOPs, initially measured by the Babinet-Soleil compensator (BSC), has been introduced to the system. Some examples of the detected signal $U2(t)$ from the FOPA are shown in Fig. 7, where the bottom signatures indicate the measured SOP values. The DOP determined for used He-Ne laser was equal to 0.99 for all measured changes of SOP.

The obtained polarisation parameters calculated from Eq. (23) have shown that the FOPA is very precise. It enables measurement of SOP with the accuracy of 1.0 deg for ϕ and 4.8 deg for Δ. Such a good accuracy, better than for classical methods (using the BSC or a rotational quarter-wave plate and a polariser) is obtained using a computer method of calculation. The LPS is driven by 1.9 kHz signal and parameters investigation time is up to 100 ms, so the system can work in real time.

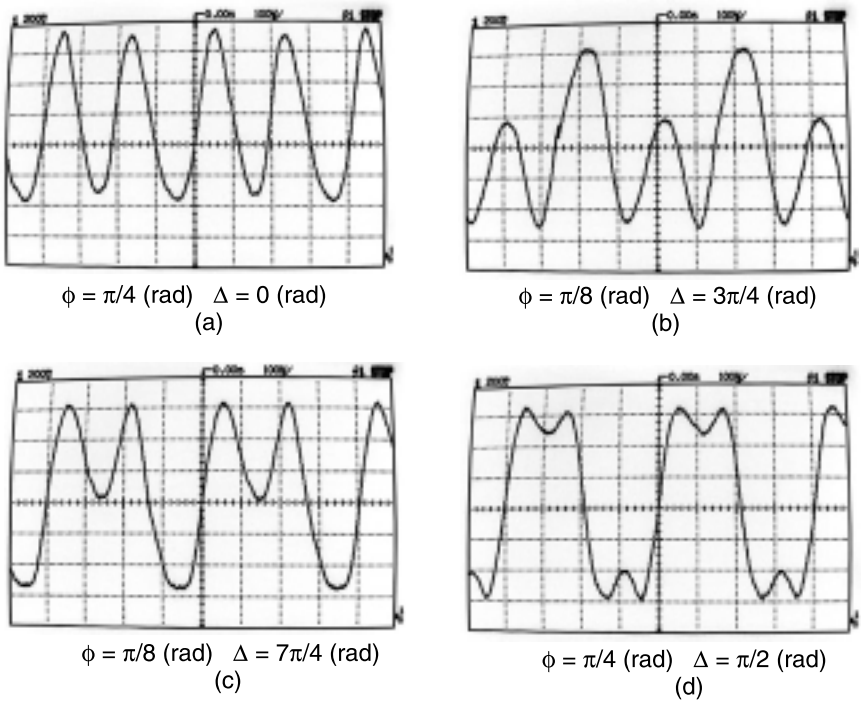

Fig. 7. Signals from the detector D2 for $P = 0.99$ and different input SOP: (a) $\phi = \pi/4$ rad, $\Delta = 0$ rad, (b) $\phi = \pi/8$ rad, $\Delta = 3\pi/4$ rad, (c) $\phi = \pi/8$ rad, $\Delta = 7\pi/4$ rad, (d) $\phi = \pi/4$ rad, $\Delta = \pi/2$ rad.

3.3. Main error sources of FOPA performance

The experiments have shown that main error sources are irregularities and instabilities of LPS element operation. The form of the modulation signal assumed in Eq. (10) is only a theoretical one. In practice, the initial deformation of the fibre by PZT squeezer should be also considered. This effect directly affects the measurement of the quantity Δ and indirectly the quantities ϕ and P due to the introduced initial constant fibre-optic birefringence. In consequence, the linear retarder describing the LPS action in the form of $\boldsymbol{G}[\delta_{in} + \delta(t)]$ with random changes of the constant value δ_{in} should be considered. Figure 8 shows some examples of the influence of random initial deformation introduced by LPS element on the system response. Unfortunately, this effect in the applied construction of LPS is difficult to eliminate.

Moreover, the LPS uses the PZT stack which needs a high voltage driving. In such a construction, the partial dissipation of the PZT squeezer driving signal $V(t)$ increases its temperature as well as the initial deformation. This source of error has influenced mainly long-term stability of the FOPA operation which is shown in Fig. 9(a). However, this disadvantage can be minimised using a fitting procedure (*Mathematica 4.1*). Measured data were fitted by linear regression procedure. The constant coefficient resulted from it gives information about an error in polarisation parameter calculation, whereas linear coefficient defines the

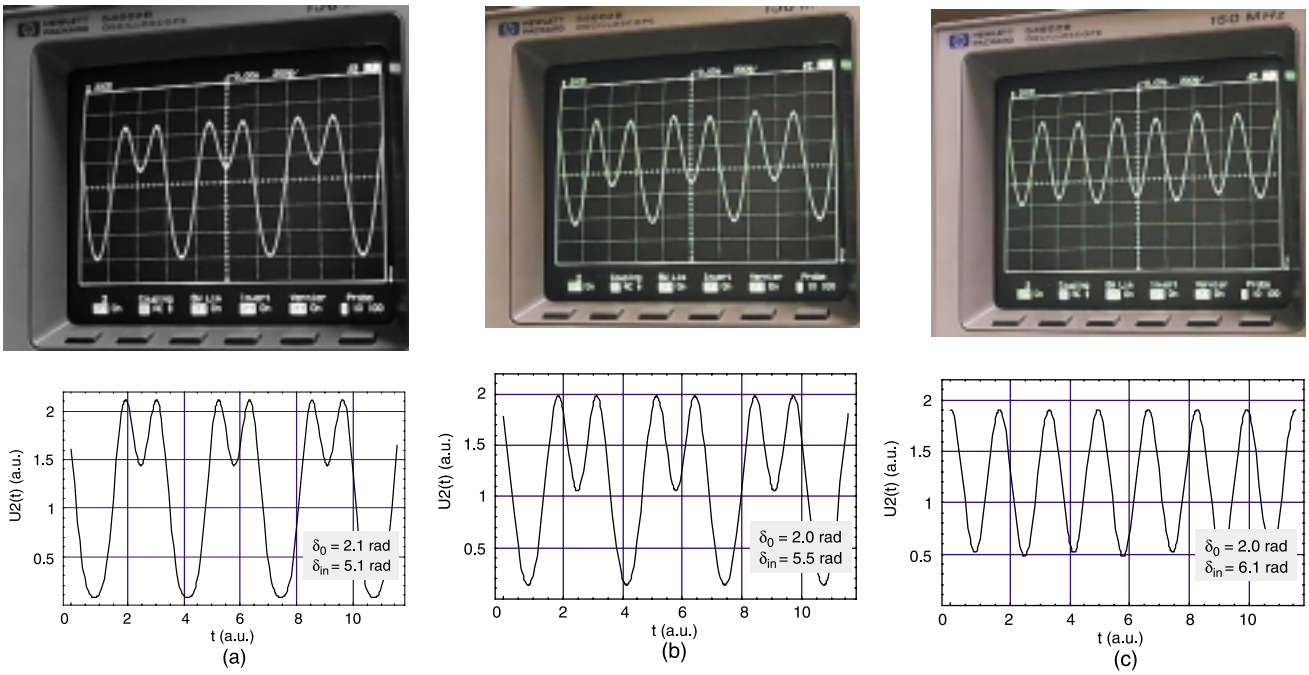

Fig. 8. Initial deformation (fibre birefringence) influence on system operation: upper – real oscillograms of the output signal $U2$, bottom – theoretically investigated signal $U2$ calculated for different δ_{in} values, respectively to the upper situation: (a) $\delta_{in} = 5.1$ rad, (b) $\delta_{in} = 5.5$ rad, and (c) $\delta_{in} = 6.1$ rad.

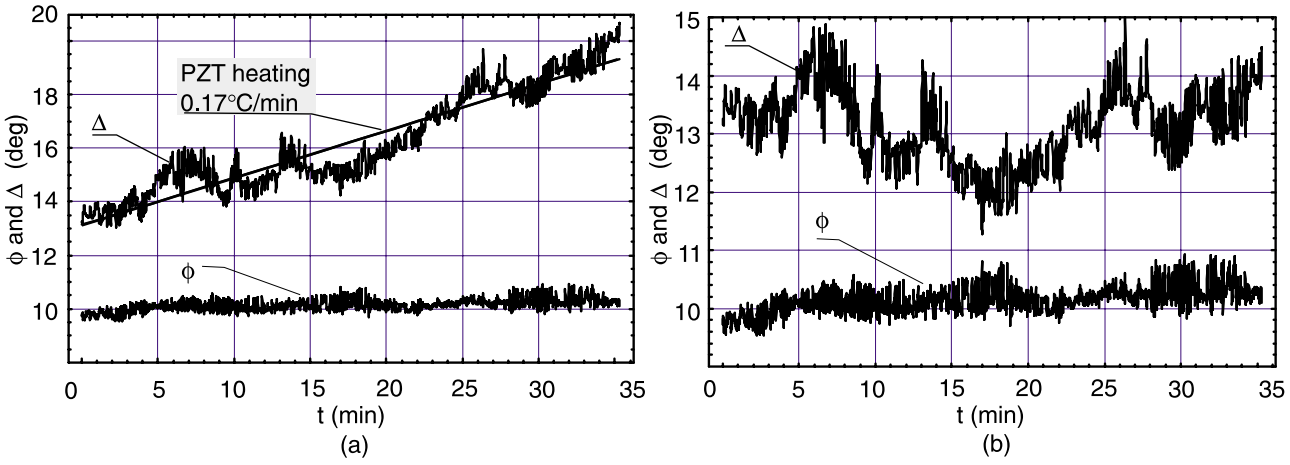

Fig. 9. Long-term stability of the FOPA system for SOP measurement: (a) before correction and (b) after correction.

temperature increasing speed, that was estimated at the rate of 0.17°C per minute. The SOP parameters can be found considering this circumstances, as it is shown in Fig. 9(b). The input SOP, measured by the BSC was Δ = 13.4 deg and ϕ = 9.8 deg, and the system drift is calculated for 1.0 deg and 4.8 deg for ϕ and Δ, respectively. These parameters directly influence the values of the system final accuracy given at the end of section 3.2.

The next source of an error of the discussed above system is a limited extinction ratio of the used fibre polarisers. As it was shown theoretically in Ref. 9, the proper system operation requires the fibre-optic polarisers with extinction ratio better than 20 dB.

4. Conclusions

The light in the optical fibre system is quasi-monochromatic and partially polarised, so the measurement of DOP as well as SOP are important. The presented in-line fibre-optic polarisation analyser ensures measurements of those parameters without implementation of rotating parts, so it is compatible with fibre-optic sensors of interferometric and polarimetric type. As a result, the in-line construction of the FOPA can be easily implemented in fibre links in the form of simple and compact devices. Because the operation frequency is about 1–2 kHz, there is a possibility of investigation of parameters up to 100 ms, so the system can work in real time. In consequence, the FOPA can be useful in some types of practical applications.

Numerical simulation as well as experimental results show that the presented system works correctly for partially polarised light. Theoretical considerations show that the system gives constant output signals for depolarised light, so Eq. (16) cannot be used. On the other hand, the parameters describing SOP do not exist when $P = 0$. It is noticeable that for quasi-monochromatic light and ideal fibre-optic polarisers, the theoretical relation of Eq. (13) and final Eq. (16) are compatible with those presented previously for polarised light in FOPE system.

The reference arm is required only for an initial adjustment of FOPA operation. Afterwards the signal from this arm is not used, but such an adjustment is needed after changing the experiment conditions. The presented results have also shown a good accuracy of the presented device in comparison with the one obtained using a classical bulk optic system. However, the applied construction of LPS element is thermally instable, very sensitive to initial squeezing and requires high voltage driving. As a consequence, this element should be optimised from the point of view of its future applications.

Acknowledgements

The authors would like to thank Dr. R. Świłło for his helpful advice. This work has been done under financial support of the State Committee for Scientific Research grant No 8T10C 042 19 and MUT statutory activity No PBS-636.

References

1. B. Henderson, "Spectroscopic measurement" in *Handbook of Optics*, 2nd edition, edited by M. Bass, pp. 20.1–30, McGrow-Hill, New York, 1995.
2. K.A. Bush, G.A. Crockett, and C.C. Bernard, "Satellite discrimination from active and passive polarisation signatures: simulation predictions using the TASAT satellite model", *Proc. SPIE* **4481**, 46–57 (2001).
3. D.H. Goldstein, D.B. Chenault, M.G. Gulley, and K.D. Spradley, "Near-infrared imaging polarimetry", *Proc. SPIE* **4481**, 100–108 (2001).
4. M.J. Duggin and R.S. Loe, "Algorithms for discrimination and contrast enhancement using narrowband polarimetric image data", *Proc. SPIE* **4481**, 247–256 (2001).
5. S.N. Shribak, "Fiber optic sensor for birefringence", *Proc. SPIE* **4481**, 175–179 (2001).
6. B. Culshaw and J. Dakin, *Optical Fiber Sensors: Systems and Applications*, Artech House, INC., Norwood, 1989.
7. L.R. Jaroszewicz, A. Kieżun, and R. Świłło, "A novel all fibre optic ellipsometer", *Proc. SPIE* **3746**, 292–295 (1999).
8. A. Kieżun and L.R. Jaroszewicz, "In-line fibre-optic ellipsometer for sensors application", *Opto-Electron. Rev.* **8**, 175–180 (2000).
9. L.R. Jaroszewicz, P. Marć, and A. Kieżun, 'In-line fibre-optic ellipsometer with full polarisation analysis in real time", *Proc. SPIE* **4481**, 141–148 (2001).
10. M.J. Beran and G.B. Parrent Jr., *Theory of Partial Coherence*, Prentice-Hall, Engeewood Cliffs, New York, 1964.
11. R.C. Jones, "A new calculus for the treatment of optical systems I: Description and discussion of the calculus", *J. Opt. Soc. Am.* **31**, 488–493 (1941).
12. L.R. Jaroszewicz, "Unified description of polarisation transmission in single-mode fibre optic elements. Part I: The equivalant lumped element representations. Part II: The experimental method and measuring system", *J. Tech. Phys.* **35**, 289–317 (1994).
13. H. Hurwitz and R.C. Jones, "A new calculus for the treatment of optical systems II: Proof of three general equivalence theorems", *J. Opt. Soc. Am.* **31**, 493–499 (1941).
14. F.P. Kapron, N.F. Borrelli, and D.B. Keck, "Birefringence in dielectric optical waveguides", *IEEE J. Quan. Electr.* **QE8**, 222–225 (1972).
15. C. Tsao, *Optical Fibre Waveguide Analysis,* Oxford University Press, New York, 1992.
16. L.R. Jaroszewicz, "Polarisation behaviour of different fiber-optic interferometer configurations under temperature changes", *Opt. Appl.* **31**, 399–423 (2001).

Recent publications of OSA

Handbook of Optics, *Second Edition*
CD-ROM
Michael Bass, *Editor-in-Chief*
Eric W. Van Stryland, David R. Williams, William L. Wolfe, *Associate Editors*

This CD-ROM contains material from the most comprehensive optics reference ever published – the 3,500-page, two-volume set of the print-published Handbook of Optics, Second Edition. Prepared by over 100 specialists in the field, this CD-ROM presents basic concepts of optics as well as necessary practical material on components, devices, and materials needed to deal with almost any problem or process in optics. Packed with vivid illustrations and a wealth of data, this handbook provides not only exhaustive reference materials, but also tutorial guidance in every topic area. Users can search, view, and print information as well as import sections into any Windows-compatible word-processor. For PC use only. Nonmembers must order directly from McGraw-Hill..

Price: List – $149.00 Member – $110.00

Optical Networking
Collected Papers of the International Conferences on Optical Fiber Sensors (OFS), 1983–1997
CD-ROM

Contains the complete contents of the OFS conference series, including post-deadline papers, totaling approximately 5,500 pages of technical content. Papers are searchable by author and keywords in title. Full-text searching can also be done using the Adobe Search interface. Users can browse the full table of contents for each OFS volume, which provides hyperlinks from the paper title to the PDF file containing the complete text.

Co-published by SPIE, OSA, and lEEE/LEOS.

1998, ISBN: 0-8194-3044-7

Price: List-$115.00 Member – $85.00

Handbook of Applied Photometry
Casimer DeCusatis, *Editor*

Photometry is the branch of science that deals with the measurement of light. It is usually viewed as a subset of the broader field of radiometry, which also includes the measurement of radiation outside the visible spectrum. Much of our information about the world comes to us through light, and the observation or detection of light is perhaps one of the most fundamental processes in nature. Fundamental questions, whose answers require photometric measurements cut across many different disciplines, are discussed in this handbook.

1997, ISBN: 1-56396-416-3

Price: List – $90.00 Member – $65.00

Introduction to Surface Roughness and Scattering, Second Edition
Jean M. Bennett and Lars Mattsson, *Authors*

This acclaimed tutorial is a total reference guide for everyone who works with optics. The type of scattering is classical scattering, not inelastic such as Raman scattering. New sections include: using scanning probe microscopes, correlation methods for rougher surfaces, surface profile measurements, and scattering theories for rougher surfaces. Also, the section on area topography measurements has been completely rewritten and the instruments described are now current.

1999, ISBN: 1-55752-609-5

Price: List – $55.00 Member – $35.00

ISO 9211 Optics and Optical Instruments – Optical Coatings: A User's Guide
Rudolf Hartmann

The International Standards Organization's 9211 Optical Coating Standard took into account a variety of existing national, military, and commercial standards and practices of defining and specifying coatings. The ISO standard has become general for the international optical community. It provides an appreciation of the details necessary to specify optical coatings. The chapters of this guide are written to correspond with each part of the Standard. ISO 921's definitions, categories and standards in the areas of coatings, imperfections, optical properties, environmental durability and specific test methods, and compared with ANSI, MIL-STD, German and British specifications.

1996, ISBN: 1-55752-462-9

Price: List – $39.00 Member – $28.00

